Non-quasiparticle effects in half-metallic ferromagnets

2007 J. Phys.: Condens. Matter 19 315201

(http://iopscience.iop.org/0953-8984/19/31/315201)

IOP PUBLISHING JOURNAL OF PHYSICS: CONDENSED MATTER

J. Phys.: Condens. Matter **19** (2007) 315201 (19pp) doi:10.1088/0953-8984/19/31/315201

Non-quasiparticle effects in half-metallic ferromagnets

V Yu Irkhin[1], M I Katsnelson[2] and A I Lichtenstein[3]

[1] Institute of Metal Physics, 620219, Ekaterinburg, Russia
[2] Institute for Molecules and Materials, Radboud University Nijmegen, NL 6525 ED Nijmegen, The Netherlands
[3] Institute of Theoretical Physics, University of Hamburg, Jungiusstrasse 9, 20355 Hamburg, Germany

Received 20 October 2006, in final form 23 October 2006
Published 3 July 2007
Online at stacks.iop.org/JPhysCM/19/315201

Abstract

The unusual electronic structure of the half-metallic ferromagnets (HMF) is analysed taking account of correlation effects (electron–magnon interaction, in particular spin-polaron effects). Special attention is paid to the so-called non-quasiparticle (NQP) (incoherent) states which arise in the minority- (majority-) spin gap above (below) the Fermi level and which may make considerable contributions to the electronic properties. First-principles calculations of the NQP states in HMF within the local-density approximation plus dynamical mean field theory (LDA + DMFT) are reviewed. These states can be probed, in particular, by spin-polarized scanning tunnelling microscopy. They also lead to observable effects in core–hole spectroscopy, nuclear magnetic relaxation and contribute to the temperature dependence of impurity resistivity, etc. The peculiarities of the transport properties of three- and two-dimensional HMF are discussed, which are connected with the absence of one-magnon spin-flip scattering processes.

1. Introduction

The history of the investigations of half-metallic ferromagnets (HMF) starts from the electronic structure calculation for NiMnSb [1]; later a number of other examples were discovered, e.g. CrO_2, Fe_3O_4 and a number of Heusler alloys Co_2MnZ and RMnSb (see reviews in [2, 3]). These substances have metallic electronic structure for one spin projection (majority- or minority-spin states), but for the opposite spin direction the Fermi level lies in the energy gap [1]. For this reason HMF now attract the growing attention of researchers in connection with 'spintronics', or spin-dependent electronics [4]. The spin-up and spin-down contributions to electronic transport properties have different orders of magnitude, which can result in a huge magnetoresistance for heterostructures containing HMF [2]. Observation of the HMF electron structure by the use of a photoemission materials with technique in colossal magnetoresistance (CMR) like $La_{1-x}Sr_xMnO_3$ [5] has also considerably increased the interest in half-metallic

ferromagnetism (however, here the situation is not clear, as Andreev reflection experiments demonstrate [6]).

The peculiar band structure of HMF results in an important role for incoherent (non-quasiparticle, NQP) states which occur near the Fermi level owing to correlation effects [2]. The appearance of NQP states in the energy gap near the Fermi level [7, 8] is one of the most interesting correlation effects typical of HMF. The origin of these states is connected with 'spin-polaron' processes: the spin-down low-energy electron excitations, which are forbidden for HMF in the one-particle picture, turn out to be possible as a superposition of spin-up electron excitations and virtual magnons. The density of the NQP states vanishes at the Fermi level but increases drastically at the energy scale of the order of a characteristic magnon frequency $\overline{\omega}$. These states are of crucial importance for spin-polarized electron spectroscopy [8, 9], NMR [10] and subgap transport in ferromagnet–superconductor junctions (Andreev reflection) [11]. The existence of NQP states at the surface of HMF has been proven for the narrow-band case in [9] and for a general case in [12]; this may be important for their detection by surface-sensitive methods such as ARPES [13] or by spin-polarized scanning tunnelling microscopy [14]. Recently, the density of NQP states has been calculated from first principles for a prototype HMF, NiMnSb [15], as well as for other Heusler alloys [16], zinc-blende structure compounds [17, 18] and CrO_2 [19].

From this point of view, HMF are very interesting conceptually as a class of materials which may be convenient for treating many-body solid state physics that is essentially beyond band theory. It is accepted that many-body effects usually lead only to renormalization of the quasiparticle parameters in the sense of Landau's Fermi liquid (FL) theory, the electronic *liquid* being *qualitatively* similar to the electron *gas* (see, e.g., [20]). On the other hand, NQP states in HMF are not described by the FL theory. As an example of the highly unusual properties of NQP states, we mention that they can contribute to the T-linear term in the electron heat capacity [21, 22], despite their density at E_{F} being zero at temperature $T = 0$.

The NQP states were first considered theoretically by Edwards and Hertz [7] in work on electron–magnon interaction in a broad-band Hubbard model of itinerant electron ferromagnets. Later it was demonstrated [8] that for a *narrow-band* (infinite-U) Hubbard model the *whole* spectral weight for one spin projection belongs to NQP states, which is of crucial importance for the problem of stability of Nagaoka's ferromagnetism [23] and for adequate description of the corresponding excitation spectrum [24]. The NQP states in the s–d exchange model of magnetic semiconductors have been considered in [25]. It was shown that depending on the sign of the s–d exchange integral they can occur either only below the Fermi energy E_{F} or only above it. Later it was realized that HMF are natural substances for theoretical and experimental investigation of NQP effects [21], and a variety of these effects in electronic and magnetic properties have been considered (earlier works are reviewed in [2]). Some recent developments concerning the physical effects of NQP states in HMF are considered in the present paper.

2. Origin of non-quasiparticle states and electron spin polarization in the gap

From a theoretical point of view, the HMF are characterized by the absence of magnon decay into Stoner excitations (electron–hole pairs with the opposite spins). Therefore spin waves are well defined in the whole Brillouin zone, similar to Heisenberg ferromagnets and degenerate ferromagnetic semiconductors. Thus, unlike the usual itinerant ferromagnets, the effects of electron–magnon interactions (so-called spin-polaron effects) are not masked by Stoner excitations in the HMF and may be studied in a pure form. As we will see below, the electron–magnon scattering results in the occurrence of NQP states.

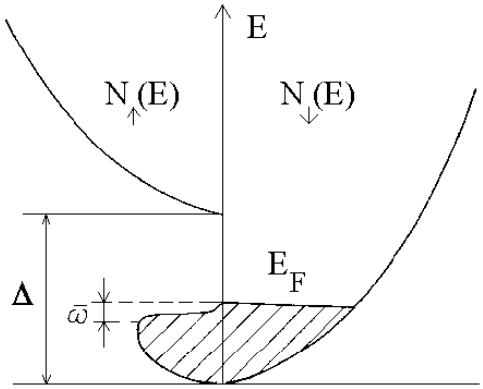

Figure 1. Density of states in a half-metallic ferromagnet with $I < 0$ (schematically). Non-quasiparticle states with $\sigma = \uparrow$ occur below the Fermi level.

We consider the interaction of charge carriers with local moments in the standard s–d exchange model

$$\mathcal{H} = \sum_{\mathbf{k}\sigma} t_{\mathbf{k}} c^{\dagger}_{\mathbf{k}\sigma} c_{\mathbf{k}\sigma} - I \sum_{\mathbf{q}\mathbf{k}\alpha\beta} \mathbf{S}_{\mathbf{q}} c^{\dagger}_{\mathbf{k}\alpha} \boldsymbol{\sigma}_{\alpha\beta} c_{\mathbf{k}-\mathbf{q}\beta} - \sum_{\mathbf{q}} J_{\mathbf{q}} \mathbf{S}_{\mathbf{q}} \mathbf{S}_{-\mathbf{q}} \tag{1}$$

where $c^{\dagger}_{\mathbf{k}\sigma}$, $c_{\mathbf{k}\sigma}$ and $\mathbf{S}_{\mathbf{q}}$ are operators for conduction electrons and localized spins in the quasimomentum representation, the electron spectrum $t_{\mathbf{k}}$ is referred to the Fermi level E_{F}, I is the s–d exchange parameter and $\boldsymbol{\sigma}$ are the Pauli matrices. The s–d exchange model does not properly describe the electronic structure for such HMF as the Heusler alloys or CrO_2, where there is no dominance of the sp-electrons in electronic transport, and a separation of electrons into a localized d-like and a delocalized s-like group is questionable. In such a case, the Hubbard model which describes the Coulomb correlations in a d-band is more appropriate. However, qualitative effects of electron–magnon interaction do not depend on the microscopic model. The calculations of the electron and magnon Green's functions in the non-degenerate Hubbard model were performed in [7, 21] and gave the same result as those in the s–d exchange model with simple replacement of I by the Hubbard parameter U.

As demonstrated by analysis of the electron-spin coupling, the NQP picture turns out to be different for two possible signs of the s–d exchange parameter I. For the case when $I < 0$, the spin-up NQP states appear below the Fermi level as an isolated region in the energy diagram (figure 1). The occupied states with total spin $S - 1$ are a superposition of the states $|S\rangle|\downarrow\rangle$ and $|S-1\rangle|\uparrow\rangle$. The entanglement of the states of electron and spin subsystems, which is necessary to form the NQP states, is a purely quantum effect that disappears in the classical limit $S \to \infty$. For a qualitative understanding of why the NQP states are formed only below the E_{F} in this case, we consider a limit $I \to -\infty$. Then the charge carrier is really a many-body state of the occupied site with total spin $S - 1/2$, which propagates in the ferromagnetic medium with spin S at all other sites. The fractions of the states $|S\rangle|\downarrow\rangle$ and $|S-1\rangle|\uparrow\rangle$ in the charge mobile carrier state are $1/(2S+1)$ and $2S/(2S+1)$, respectively, so that the first number is just a spectral weight of *occupied* spin-up electron NQP states. At the same time, the density of *empty* states is measured by the number of electrons with a given spin projection which can be added to the system. It is obvious that one cannot put any spin-up electrons in the spin-up site with $I = -\infty$. Therefore the density of NQP states should vanish above E_{F}.

On the contrary, for the $I > 0$ case, the spin-down NQP scattering states form a 'tail' of the upper spin-down band, which starts from the E_{F} (figure 2) since the Pauli principle prevents

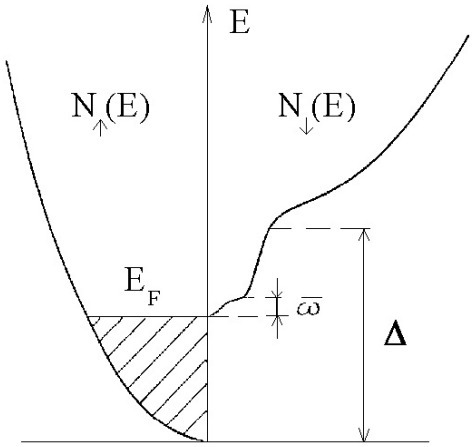

Figure 2. The density of states in a half-metallic ferromagnet with $I > 0$ (schematic). Non-quasiparticle states with $\sigma = \downarrow$ occur above the Fermi level.

electron scattering into occupied states. A similar analysis of the limit $I \to +\infty$ helps us to understand the situation qualitatively.

It is worthwhile noting that in the best known HMF an energy gap exists for minority-spin states [2], which is similar to the case $I > 0$; therefore the NQP states should arise *above* the Fermi energy. For exceptional cases with a *majority*-spin gap such as a double perovskite Sr_2FeMoO_6 [26] one should expect the NQP states *below* the Fermi energy. This prediction is very interesting since in the latter case the NQP states can be probed by spin-polarized photoemission which is technically much simpler than the spin-polarized bremsstrahlung isochromat spectroscopy (BIS) spectra [27] needed to probe the empty NQP states.

We will now consider the density of states (DOS) scheme for the HMF within the s–d exchange model more quantitatively [2, 25]. The electron Green's function has the form

$$G^{\sigma}_{\mathbf{k}}(E) = [E - t_{\mathbf{k}\sigma} - \Sigma_{\mathbf{k}\sigma}(E)]^{-1} \tag{2}$$

where $t_{\mathbf{k}\sigma} = t_{\mathbf{k}} - \sigma I \langle S^z \rangle$ is the mean-field electron spectrum and $\Sigma_{\mathbf{k}\sigma}(E)$ is the self-energy which describes the electron–magnon interaction. Within the second-order approximation in I one has $\Sigma_{\mathbf{k}\sigma}(E) = 2I^2 S Q^{\sigma}_{\mathbf{k}}(E)$ with

$$Q^{\uparrow}_{\mathbf{k}}(E) = \sum_{\mathbf{q}} \frac{N_{\mathbf{q}} + n^{\downarrow}_{\mathbf{k}+\mathbf{q}}}{E - t_{\mathbf{k}+\mathbf{q}\downarrow} + \omega_{\mathbf{q}}}, \qquad Q^{\downarrow}_{\mathbf{k}}(E) = \sum_{\mathbf{q}} \frac{1 + N_{\mathbf{q}} - n^{\uparrow}_{\mathbf{k}-\mathbf{q}}}{E - t_{\mathbf{k}-\mathbf{q}\uparrow} - \omega_{\mathbf{q}}}. \tag{3}$$

Using an expansion of the Dyson equation (2) we obtain a simple expression for the electron DOS

$$N_{\sigma}(E) = \sum_{\mathbf{k}} \delta(E - t_{\mathbf{k}\sigma}) - \sum_{\mathbf{k}} \delta'(E - t_{\mathbf{k}\sigma}) \operatorname{Re} \Sigma_{\mathbf{k}\sigma}(E) - \frac{1}{\pi} \sum_{\mathbf{k}} \frac{\operatorname{Im} \Sigma_{\mathbf{k}\sigma}(E)}{(E - t_{\mathbf{k}\sigma})^2}. \tag{4}$$

The second term on the right-hand side of equation (4) describes the renormalization of quasiparticle energies. The third term, which arises from the branch cut of the self-energy $\Sigma_{\mathbf{k}\sigma}(E)$, describes the incoherent (NQP) contribution owing to scattering by magnons. One can see that the NQP DOS does not vanish in the energy region, corresponding to the 'alien' spin subband with the opposite projection $-\sigma$. Substituting equation (3) into equation (4) and

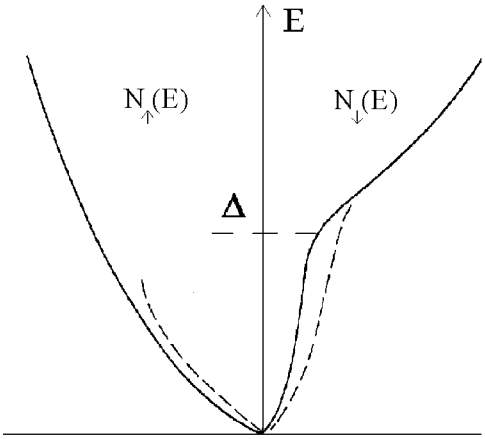

Figure 3. Density of states in the s–d model in the case of an empty conduction band ($I > 0$). At $T = 0$ (solid line) the spin-polaron tail of spin-down states reaches the bottom of the band. The dashed line corresponds to finite temperatures.

neglecting the quasiparticle shift we obtain for the case of HMF with $I > 0$

$$N_\uparrow(E) = \sum_{\mathbf{kq}} \left[1 - \frac{2I^2 S N_\mathbf{q}}{(t_{\mathbf{k}+\mathbf{q}\downarrow} - t_{\mathbf{k}\uparrow})^2}\right] \delta(E - t_{\mathbf{k}\uparrow})$$
$$N_\downarrow(E) = 2I^2 S \sum_{\mathbf{kq}} \frac{1 + N_\mathbf{q} - n_{\mathbf{k}\uparrow}}{(t_{\mathbf{k}+\mathbf{q}\downarrow} - t_{\mathbf{k}\uparrow} - \omega_\mathbf{q})^2} \delta(E - t_{\mathbf{k}\uparrow} - \omega_\mathbf{q}). \tag{5}$$

The DOS for case of the empty conduction band is shown in figure 3. The $T^{3/2}$ dependence of the magnon contribution to the residue of the Green's function (2), which follows from (3), i.e. of the effective electron mass in the lower spin subband, and an increase with temperature of the incoherent tail from the upper spin subband result in a strong temperature dependence of the partial densities of states $N_\sigma(E)$, the corrections being of opposite sign.

The $N(E)$ behaviour near the Fermi level in the HMF (or degenerate ferromagnetic semiconductor) turns out also to be non-trivial (figures 2 and 3). Provided that we neglect magnon frequencies in the denominators of equation (5), the partial density of incoherent states should occur as a jump above or below the Fermi energy E_F for the case of $I > 0$ and $I < 0$, respectively, owing to the Fermi distribution functions. An account of finite magnon frequencies $\omega_\mathbf{q} = Dq^2$ (D is the spin stiffness constant) leads to smearing of these singularities on the energy interval $\overline{\omega} \ll E_\mathrm{F}$, $N_\alpha(E_\mathrm{F})$ being equal to zero. For $|E - E_\mathrm{F}| \ll \overline{\omega}$ we obtain

$$\frac{N_{-\alpha}(E)}{N_\alpha(E)} = \frac{1}{2S} \left|\frac{E - E_\mathrm{F}}{\overline{\omega}}\right|^{3/2} \theta(\alpha(E - E_\mathrm{F})), \tag{6}$$

where $\alpha = \operatorname{sgn} I = \pm 1$ are the spin projections $\uparrow, \downarrow$ of corresponding quasiparticle states. With increasing $|E - E_\mathrm{F}|$, $N_{-\alpha}/N_\alpha$ tends to a constant value which is of the order of I^2 within the perturbation theory. In the strong coupling limit where $|I| \to \infty$ we have for $|E - E_\mathrm{F}| \gg \overline{\omega}$

$$\frac{N_{-\alpha}(E)}{N_\alpha(E)} = \frac{1}{2S} \theta(\alpha(E - E_\mathrm{F})). \tag{7}$$

To treat details of the energy dependence of $N(E)$ in the broad-band case, we assume the simplest isotropic approximation for the majority-spin electrons,

$$t_{\mathbf{k}\uparrow} - E_\mathrm{F} \equiv \xi_\mathbf{k} = \frac{k^2 - k_\mathrm{F}^2}{2m^*}. \tag{8}$$

Provided that we use the rigid splitting approximation $t_{\mathbf{k}\downarrow} = t_{\mathbf{k}\uparrow} + \Delta$ ($\Delta = 2IS, I > 0$), the half-metallic situation (or, more precisely, the situation of a degenerate ferromagnetic semiconductor) takes place for $\Delta > E_{\mathrm{F}}$. Then qualitatively the equation (6) works to the accuracy of a prefactor. It is worth noting that, formally speaking, the NQP contribution to DOS also occurs for a usual metal where $\Delta < E_{\mathrm{F}}$. In the case of small Δ there is a crossover energy (or temperature) scale

$$T^* = D(m^*\Delta/k_{\mathrm{F}})^2 \tag{9}$$

which is the magnon energy at the boundary of the Stoner continuum, $T^* \simeq \overline{\omega}(\Delta/E_{\mathrm{F}})^2 \ll \overline{\omega}$.

The model of rigid spin splitting used above is in fact not applicable for real HMF systems where the gap has a hybridization origin [1, 2]. The simplest model for HMF is as follows: a 'normal' metallic spectrum for majority electrons (8) and the hybridization gap for minority ones,

$$t_{\mathbf{k}\downarrow} - E_{\mathrm{F}} = \tfrac{1}{2}\left(\xi_{\mathbf{k}} + \mathrm{sgn}\,(\xi_{\mathbf{k}})\sqrt{\xi_{\mathbf{k}}^2 + \Delta^2}\right). \tag{10}$$

Here we assume for simplicity that the Fermi energy lies exactly in the middle of the hybridization gap (otherwise one needs to shift $\xi_{\mathbf{k}} \to \xi_{\mathbf{k}} + E_0 - E_{\mathrm{F}}$ in the last equation, E_0 being the middle of the gap). In equation (5) one can replace $\xi_{\mathbf{k}+\mathbf{q}}$ by $\mathbf{v}_{\mathbf{k}}\mathbf{q}$, $\mathbf{v}_{\mathbf{k}} = \mathbf{k}/m^*$. Integrating over the angle between the vectors $\mathbf{k}$ and $\mathbf{q}$ we derive

$$\left\langle\left(\frac{1}{t_{\mathbf{k}+\mathbf{q}\downarrow} - t_{\mathbf{k}\uparrow} - \omega_{\mathbf{q}}}\right)^2\right\rangle = \frac{8}{v_{\mathrm{F}}q\Delta}\left(\frac{2}{3}\left[X^3 - (X^2+1)^{3/2} + 1\right] + X\right) \tag{11}$$

where angular brackets stand for the average over the angles of the vector $\mathbf{k}$, $X = k_{\mathrm{F}}q/m^*\Delta$. Here we do have the crossover with the energy scale T^* which can be small for a small enough hybridization gap. For example, in NiMnSb the conduction band width is about 5 eV and the distance from the Fermi level to the nearest gap edge (i.e. the indirect energy gap which is proportional to Δ^2) is smaller than 0.5 eV, so that $(\Delta/E_{\mathrm{F}})^2 \leqslant 0.1$.

For the case $0 < E - E_{\mathrm{F}} \ll \overline{\omega}$ one has [12]

$$\begin{aligned} &N_\downarrow(E) \propto b\left(\frac{E - E_{\mathrm{F}}}{T^*}\right), \\ &b(y) = \tfrac{2}{5}\left[y^{5/2} - (1+y)^{5/2} + 1\right] + y + y^{3/2} \simeq \begin{cases} y^{3/2}, & y \ll 1 \\ y, & y \gg 1. \end{cases} \end{aligned} \tag{12}$$

Thus the behaviour $N_\downarrow(E) \propto (E - E_{\mathrm{F}})^{3/2}$ takes place only for very small excitation energies $E - E_{\mathrm{F}} \ll T^*$, whereas in a broad interval $T^* \ll E - E_{\mathrm{F}} \ll \overline{\omega}$ one has the linear dependence $N_\downarrow(E) \propto E - E_{\mathrm{F}}$.

In a simple s–d model case, qualitative considerations [28], as well as formal Green's functions calculations [25, 29], give a spin polarization of conduction electrons in the spin-wave region which is proportional to magnetization:

$$P \equiv \frac{N_\uparrow - N_\downarrow}{N_\uparrow + N_\downarrow} = P_0\frac{\langle S^z\rangle}{S}. \tag{13}$$

A weak ground-state depolarization $1 - P_0$ occurs in the case where $I > 0$. The behaviour $P(T) \simeq \langle S^z\rangle/S$ is qualitatively confirmed by experimental data on field emission for ferromagnetic semiconductors [30] and transport properties for the half-metallic Heusler alloys [31].

An attempt to generalize the result (13) to the HMF case has been made on the basis of qualitative arguments for the atomic limit [32]. We will demonstrate that the situation for

the HMF is more complicated. Let us focus on the magnon contribution to the DOS (5) and calculate the following function:

$$\Lambda = \sum_{\mathbf{kq}} \frac{2I^2 S N_{\mathbf{q}}}{(t_{\mathbf{k}+\mathbf{q}\downarrow} - t_{\mathbf{k}\uparrow} - \omega_{\mathbf{q}})^2} \delta(E_{\mathrm{F}} - t_{\mathbf{k}\uparrow}). \tag{14}$$

Using the parabolic electron spectrum $t_{\mathbf{k}\uparrow} = k^2/2m^*$ and averaging over the angles of the vector $\mathbf{k}$ we obtain

$$\Lambda = \frac{2I^2 S m^2}{k_{\mathrm{F}}^2} \rho \sum_{\mathbf{q}} \frac{N_{\mathbf{q}}}{(q_0)^2 - q^2} \tag{15}$$

where $\rho = N_\uparrow(E_{\mathrm{F}}, T = 0)$, and we have used the condition $q \ll k_{\mathrm{F}}$, $q_0 = m^*\Delta/k_{\mathrm{F}} = \Delta/v_{\mathrm{F}}$, $\Delta = 2|I|S$ being the spin splitting. In a ferromagnetic semiconductor we have, in agreement with the qualitative considerations presented above:

$$\Lambda = \frac{S - \langle S^z \rangle}{2S} \rho \propto \left(\frac{T}{T_{\mathrm{C}}}\right)^{3/2} \rho. \tag{16}$$

Later we consider the spectrum model (8), (10) where the gap has a hybridization origin. At $T \ll T^*$ we reproduce the result (16) which is actually universal for this temperature region. At $T^* \ll T \ll \overline{\omega}$ we derive

$$\Lambda \propto q_0 \sum_{\mathbf{q}} \frac{N_{\mathbf{q}}}{q} \propto \frac{T^{*1/2}}{T_{\mathrm{C}}^{1/2}} T \ln \frac{T}{T^*}. \tag{17}$$

This result distinguishes HMF like the Heusler alloys from ferromagnetic semiconductors and narrow-band saturated ferromagnets. In the narrow-band case the spin polarization follows the magnetization up to the Curie temperature T_{C}.

For finite temperatures the density of NQP states at the Fermi energy is proportional to [22, 25, 28]

$$N(E_{\mathrm{F}}) \propto \int_0^\infty \mathrm{d}\omega \, \frac{K(\omega)}{\sinh(\omega/T)}. \tag{18}$$

Generally, for temperatures which are comparable with the Curie temperature T_{C} there are no essential differences between half-metallic and 'ordinary' ferromagnets since the gap is filled. The corresponding symmetry analysis is performed in [22] for a model of conduction electrons interacting with 'pseudospin' excitations in ferroelectric semiconductors. The symmetrical (with respect to E_{F}) part of $N(E)$ in the gap can be attributed to smearing of electron states by electron–magnon scattering; the asymmetrical ('Kondo-like') one is the density of NQP states owing to the Fermi distribution function. Note that this filling of the gap is very important for possible applications of HMF in spintronics: they really have some advantages only provided that $T \ll T_{\mathrm{C}}$. Since a single-particle Stoner-like theory leads to a much less restrictive (but unfortunately completely wrong) inequality $T \ll \Delta$, a many-body treatment of the spin-polarization problem (inclusion of collective spin-wave excitations) is required.

Even though the NQP states do not contribute to DOS at the Fermi level, they can contribute to the linear term in the heat capacity [21, 22]. This fact is connected with a subtle difference between dynamical quasiparticles in an interacting Fermi system, which are described by the Green's function poles, and the statistical quasiparticles in a sense of Landau Fermi liquid theory [20]. This issue is discussed in detail in [2, 21].

3. First-principles calculations of non-quasiparticle states: a dynamical mean field theory

A history of the HMF starts from the band structure of the semi-Heusler alloy NiMnSb [1]. Since then numerous first-principles electronic structure investigations of HMF have been carried out (see, e.g., recent papers [33–36] and a review of early works in [2]). They were based on a standard local density approximation (LDA) or generalized gradient approximation (GGA) to the density functional theory, and, sometimes, on the LDA + U approximation (see [37] for CrO_2). Of course, essential correlation effects such as NQP states cannot be considered with these techniques.

Recently, a successful approach has been proposed [38, 39] to include correlation effects into the first-principles electronic structure calculations by combining the LDA scheme with the dynamical mean-field theory (DMFT). The DMFT maps a lattice many-body system onto quantum impurity models under a self-consistency condition (for a review, see [40]). In this way, the complex lattice many-body problem splits into a simple one-body crystal problem with a local self-energy and the effective many-body impurity problem. In a sense, the approach is complementary to the local density approximation [41–43] where the many-body problem splits into a one-body problem for a crystal and a many-body problem for *homogeneous* electron gas. Naively speaking, the LDA + DMFT method [38, 39] treats localized d- and f-electrons in the spirit of the DMFT and delocalized s, p-electrons in the spirit of the LDA. Thanks to numerical and analytical techniques developed for solution of the effective quantum-impurity problem [40], the DMFT becomes a very efficient and extensively used approximation for local energy-dependent self-energy $\Sigma(\omega)$. The accurate LDA + DMFT scheme can be used for calculating a large number of systems with electron correlations of different strengths (for a detailed description of the method and computational results see [44–47]). Following the work in [15] we present here the first LDA + DMFT results for the electronic structure calculations of a 'prototype' HMF NiMnSb as an example. The LDA + DMFT calculations have been carried out for HMF in [16–19, 48]. In particular, it was demonstrated that taking into account the correlation effects by this method significantly improves the agreement between theory and experiment for the magneto-optical properties of NiMnSb, in comparison with the LDA/GGA [48].

Before considering the real HMF case, it is worthwhile discussing the applicability of the DMFT scheme for quantitative description of the NQP states. The DMFT is considered as an *optimal* local approximation which means that the self-energy depends only on the energy and not on the quasimomentum [40]. At the same time, the NQP states are connected with the self-energy (3) which is almost local. It will be *exactly* local if we neglect magnon energies in comparison with the electron bandwidth, which is a rather accurate approximation for realistic parameters. The local approximation means formally that we replace the **q**-dependent magnon spectral density by the average one, as in equation (18). It should be stressed that an accurate description of the *magnon* spectrum is not important for the existence of the NQP states, nor for proper estimation of their spectral weight, but can be important for an explicit shape of the DOS tail in the vicinity of the Fermi level (see equation (6)).

We start from the DMFT calculations for the one-band Hubbard Hamiltonian

$$H = -\sum_{i,j,\sigma} t_{ij}(c^{\dagger}_{i\sigma}c_{j\sigma} + c^{\dagger}_{j\sigma}c_{i\sigma}) + U\sum_{i} n_{i\uparrow}n_{i\downarrow}, \tag{19}$$

on the Bethe lattice with coordination $z \to \infty$ and nearest-neighbour hopping $t_{ij} = t/\sqrt{z}$ (in this limit the DMFT is formally exact [40]). In this case the DOS has a semi-elliptic form. In order to stabilize the HMF state in our toy model, we have added an external magnetic spin splitting Δ, which mimics the local Hund polarization from other electrons in the real NiMnSb

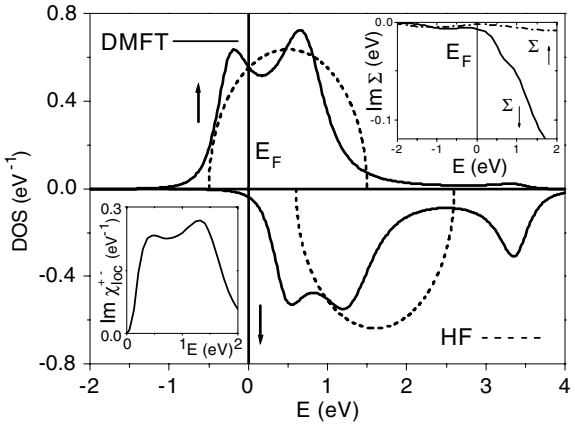

Figure 4. Density of states for HMF in the Hartree–Fock (HF) approximation (dashed line) and the QMC solution of the DMFT problem for a semi-circular model (solid line) with the band width $W = 2$ eV, Coulomb interaction $U = 2$ eV, spin splitting $\Delta = 0.5$ eV, chemical potential $\mu = -1.5$ eV and temperature $T = 0.25$ eV. Insets: imaginary part of the local spin-flip susceptibility (left) and the spin-resolved self-energy (right).

compound. This HMF state corresponds to a mean-field (Hartree–Fock) solution with a LSDA-like DOS (figure 4).

We can study an average magnon spectrum in this model through the two-particle correlation function. The local spin-flip susceptibility

$$\chi^{+-}_{\mathrm{loc}}(\tau) = \langle S^{+}(\tau)S^{-}(0)\rangle = \langle c^{\dagger}_{\uparrow}(\tau)c_{\downarrow}(\tau)c^{\dagger}_{\downarrow}(0)c_{\uparrow}(0)\rangle, \tag{20}$$

represents the response function required. We have calculated this function using the numerically exact QMC procedure [49].

The model DMFT results are presented in figure 4. In comparison with a simple Hartree–Fock solution (dashed line) one can see additional well-pronounced states that appear in the spin-down gap region, just above the Fermi level. This new many-body feature corresponds to the NQP states. In addition to these states which are visible in both spin channels of the DOS around 0.5 eV, a many-body satellite appears at an energy of 3.5 eV.

The left inset in the figure 4 represents the imaginary part of the local spin-flip susceptibility. One can see a well pronounced shoulder (around 0.5 eV), which is connected with an average magnon DOS. In addition there is a broad maximum (at 1 eV) corresponding to the Stoner excitation energy. The right inset in the figure 4 represents the imaginary part of the self-energy calculated from our 'toy model'. The spin-up channel can be described by a Fermi liquid type behaviour with a parabolic energy dependence $-\operatorname{Im}\Sigma^{\uparrow} \propto (E - E_{\mathrm{F}})^2$, whereas in the spin-down channel the imaginary part $-\operatorname{Im}\Sigma^{\downarrow}$ shows the 0.5 eV NQP shoulder. Due to the relatively high temperature of our QMC calculation (an exact enumeration technique with the number of time slices equal to $L = 24$) the NQP tail goes a bit below the Fermi level, in agreement with equation (18); at temperature $T = 0$ the NQP tail should end exactly at the Fermi level.

Let us move to the calculations for a real NiMnSb. The details of the computational scheme have been described in [15], and only the key points will be mentioned here. In order to integrate the DMFT approach into the band structure calculation the so-called exact muffin-tin orbital method (EMTO) [50, 51] was used. In the EMTO approach, the effective one-electron potential is represented by the optimized overlapping muffin-tin potential, which is the best

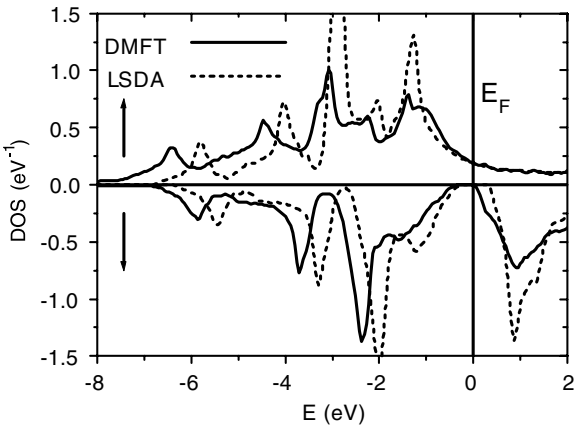

Figure 5. Density of states for the HMF NiMnSb in the LSDA scheme (dashed line) and in the LDA + DMFT scheme (solid line) with effective Coulomb interaction $U = 3$ eV, exchange parameter $J = 0.9$ eV and temperature $T = 300$ K. The NQP states are evidenced just above the Fermi level.

possible spherical approximation to the full one-electron potential. The implementation of the DMFT scheme in the EMTO method is described in detail in [52]. In addition to the usual self-consistency of the many-body problem (self-consistency of the self-energy), a charge self-consistency was achieved [47].

For the interaction Hamiltonian, a most general rotationally invariant form of the generalized Hubbard model has been used [39]. The effective many-body impurity problem is solved using the spin-polarized T-matrix plus fluctuation-exchange approximation (a so-called SPTF) scheme proposed in [53], which is a development of the earlier approach [39]. The SPTF approximation is a multiband spin-polarized generalization of a well-known fluctuation exchange (FLEX) approximation [54], but with a different treatment of the particle–hole (PH) and particle–particle (PP) channels. The PP channel is described by a T-matrix approach [55] yielding a renormalization of the effective interaction. The static part of this effective interaction is used explicitly in the PH channel.

There are various methods for estimating the required values of the on-site Coulomb repulsion energy U and exchange interaction parameter J for real materials. The constrained LDA calculation [56] estimates an average Coulomb interaction between the Mn d-electrons as $U = 4.8$ eV with an exchange interaction of $J = 0.9$ eV. However, this method is adequate for typical insulating screening but in general not accurate for a metallic kind of screening. The latter will lead to a smaller value of U. Unfortunately, there are no reliable schemes for calculating U for metals; therefore the results for different values of U in the energy interval from 0.5 eV to the constrained LDA value $U = 4.8$ eV have been tested. At the same time, the results of constrained LDA calculations for the Hund exchange parameter J do not depend on metallic screening and should be reliable enough. It turns out that the LDA + DMFT results are not very sensitive to the value of U due to the T-matrix renormalization. Figure 5 represents the results for DOS using LSDA and LDA + DMFT (with $U = 3$ eV and $J = 0.9$ eV) approaches.

It is important to mention that the magnetic moment per formula unit is not sensitive to the U values and equals exactly $\mu = 4\ \mu_B$, which suggests that the half-metallic state is stable with respect to introducing the correlation effects. In addition, the DMFT gap in the spin-down channel, defined as the distance between the occupied part and the starting point of the NQP 'tail', is also not very sensitive to the U values. For different U values the slope of the

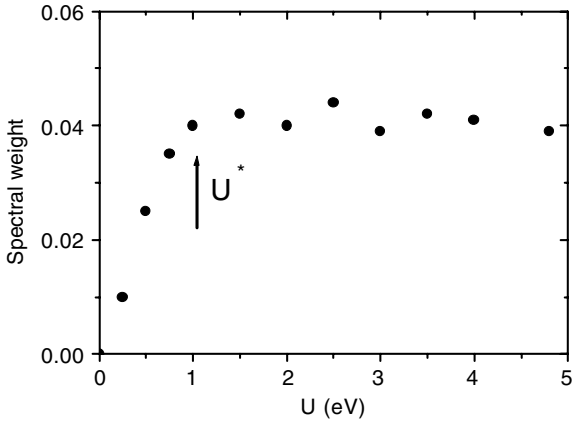

Figure 6. Spectral weight of the non-quasiparticle states calculated as a function of average on-site Coulomb repulsion U at $T = 300$ K.

'tail' is slightly changed, but the total DOS is weakly U-dependent due to the same T-matrix renormalization effects.

Thus the correlation effects do not influence the general features of the electron energy spectrum too strongly (except for smearing of the DOS which is due to the finite temperature $T = 300$ K in our calculations). The only qualitatively new effect is the appearance of a tail of the NQP states in the energy gap above the Fermi energy. The NQP spectral weight for realistic values of the parameters is not very small, which means that the NQP states should be well pronounced in the corresponding experimental data. A relatively weak dependence of the NQP spectral weight on the U value (figure 6) is also a consequence of the T-matrix renormalization [53]. One can see that T-matrix depends slightly on U provided that the latter is larger than the widths of the main DOS peaks near the Fermi level in the energy range of 2 eV (this is of the order of $U^* \simeq 1$ eV).

For the spin-up states we have a normal Fermi-liquid behaviour $-\operatorname{Im}\Sigma_d^{\uparrow}(E) \propto (E - E_{\mathrm{F}})^2$ with a typical energy scale of the order of several eV. The spin-down self-energy behaves in a similar way below the Fermi energy, with a slightly smaller energy scale (which is still larger than 1 eV). At the same time, a significant increase in $\operatorname{Im}\Sigma_d^{\downarrow}(E)$ with a much smaller energy scale (a few tenths of an eV) takes place just above the Fermi level, which is more pronounced for t_{2g} states (figure 7). A similar behaviour of the imaginary part of the electronic self-energy and the DOS just above the Fermi level is a manifestation of the NQP states and is also noticed in the model calculation (figure 4).

Thus the main results of [15] are (i) the existence of the NQP states in the real electronic structure of a specific compound and (ii) estimation of their spectral weight in the LDA + DMFT approach. The temperature dependence of the NQP density of states in the gap, which is important for possible applications of the HMF in spintronics, was analysed by this technique in [16].

4. X-ray absorption and emission spectra. Resonant x-ray scattering

To treat many-body effects in the electron energy spectrum of HMF with lattice defects, one can use the s–d exchange model in the presence of the potential $\mathcal{U}$ induced by the impurity at a lattice site, which can be written down in the representation of the exact eigenfunctions [12].

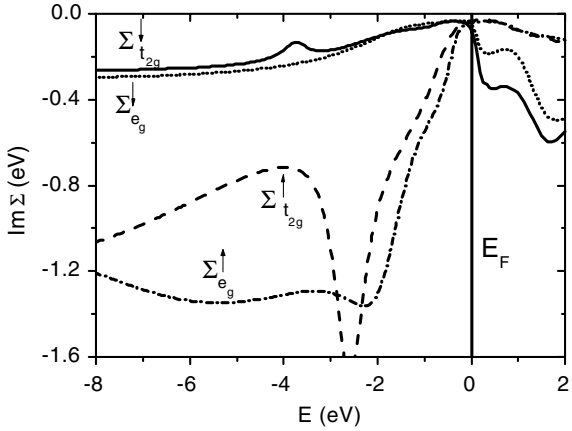

Figure 7. The imaginary part of self-energies Im $\Sigma_d^{\downarrow}$ for t_{2g} (solid line) and e_g (dotted line), Im $\Sigma_d^{\uparrow}$ for t_{2g} (dashed line) and e_g (dashed–dotted line), respectively.

The impurity potential results in the NQP contribution to this quantity being enhanced for $\mathcal{U} < 0$ and suppressed for $\mathcal{U} > 0$. This consideration is also relevant to treat the manifestations of NQP states in the core level spectroscopy where the core–hole potential is important [57]. Various spectroscopic techniques such as x-ray absorption, x-ray emission and photoelectron spectroscopies (XAS, XES and XPS, respectively) give important information about the electronic structure of HMF and related compounds, i.e. ferromagnetic semiconductors and colossal magnetoresistance materials (see, e.g., [58–61]). It is well known [62] that many-body effects (e.g. dynamical core–hole screening) can be important for the core level spectroscopy even when the system is not strongly correlated in the initial state. Therefore it is instructive to study the interplay of these effects and NQP states which are of essentially of many-body origin themselves.

To consider the core level problem in HMF we use the Hamiltonian of the s–d exchange model in the presence of the external potential $\mathcal{U}$ induced by the core–hole

$$\mathcal{H}' = \varepsilon_0 f^\dagger f + \mathcal{U} \sum_{\mathbf{k}\mathbf{k}'\sigma} c^\dagger_{\mathbf{k}\sigma} c_{\mathbf{k}'\sigma} f^\dagger f \tag{21}$$

where $f^\dagger$, f are core–hole operators and $\mathcal{U} < 0$. X-ray absorption and emission spectra are determined by the two-particle Green's function [62]

$$G^\sigma_{\mathbf{k}\mathbf{k}'}(E) = \langle\langle c_{\mathbf{k}\sigma} f | f^\dagger c^\dagger_{\mathbf{k}'\sigma}\rangle\rangle_E. \tag{22}$$

Thus the core–hole problem is formally similar to the impurity problem. Since XAS probes empty states and XES occupied states, the local DOS

$$N^\sigma_{\mathrm{loc}}(E) = -\frac{1}{\pi} \operatorname{Im} G^\sigma_{00}(E) \tag{23}$$

describes the absorption spectrum for $E > E_{\mathrm{F}}$ and the emission spectrum for $E < E_{\mathrm{F}}$. To take into account the core level broadening a finite damping δ should be introduced [57]. For small band filling the 'exciton effects' (strong interaction with the core–hole) result in a considerable enhancement of NQP contributions to the spectra in comparison with those to DOS. The results for a semi-elliptic bare band are shown in figures 8 and 9.

To probe the spin-polaron nature of the NQP states more explicitly, it would be desirable to use spin-resolved spectroscopic methods such as x-ray magnetic circular dichroism (XMCD; for a review see [63]). Owing to interference of electron–magnon scattering and exciton effects

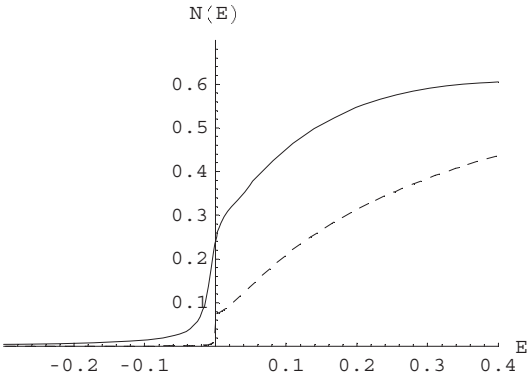

Figure 8. The local density of states $N^{\uparrow}_{\rm loc}(E)$ (solid line) for a HMF with $S = 1/2$, $I = 0.3$, $\delta = 0.01$ in the presence of the core–hole potential $\mathcal{U} = -0.2$. The dashed line shows the DOS $N_{\uparrow}(E)$ for the ideal crystal. The value of $E_{\rm F}$ calculated from the band bottom is 0.15.

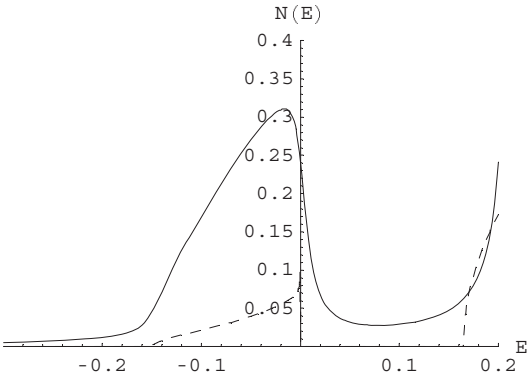

Figure 9. The local density of states $N^{\uparrow}_{\rm loc}(E)$ (solid line) for a HMF with $S = 1/2$, $I = -0.3$, $\delta = 0.01$ in the presence of the core–hole potential $\mathcal{U} = -0.3$. The dashed line shows the DOS $N_{\uparrow}(E)$ for the ideal crystal. The value of $E_{\rm F}$ calculated from the band bottom is 0.15.

(interaction of electrons with the core–hole), the NQP contributions to x-ray spectra can be considerably enhanced in comparison with contributions to the DOS of the ideal crystal. Thus core level (XAS, XES and XPS) spectroscopy might be an efficient tool for investigating the NQP states in the electron energy spectrum.

Now we consider NQP effects in resonant x-ray scattering processes. The intensity of resonant x-ray emission induced by a photon with the energy ω and polarization q is given by the Kramers–Heisenberg formula (see, e.g., reference [64])

$$I_{q'q}(\omega', \omega) \propto \sum_n \left| \sum_l \frac{\langle n|C_{q'}|l\rangle\langle l|C_q|0\rangle}{E_0 + \omega' - E_l - {\rm i}\Gamma_l} \right|^2 \delta(E_n + \omega' - E_0 - \omega). \qquad (24)$$

Here q' and ω' are the polarization and energy of the emitted photon, $|n\rangle$, $|0\rangle$ and $|l\rangle$ are the final, initial and intermediate states of the scattering system, respectively, E_i are the corresponding energies, C_q is the operator of the dipole moment for the transition, which is proportional to $fc + c^{\dagger}f^{\dagger}$. Assuming for simplicity that Γ_l does not depend on the intermediate state, $\Gamma_l = \Gamma$, and taking into account only the main x-ray scattering channel (where the hole

is filled from the conduction band) one obtains [65]

$$I_{\omega'} \propto \left| \sum_{\sigma} G^{\sigma}_{00}(z) \right|^2 \tag{25}$$

where $z = \omega' - E_0 + \mathrm{i}\Gamma$. Owing to a jump in the DOS at the Fermi level, the NQP part of the Green's function contains a large logarithm $\ln(W/z)$ at small z. This means that the corresponding contribution to the elastic x-ray scattering intensity ($\omega' = E_0$) is enhanced by a factor $\ln^2(W/\Gamma)$. Recently [60] the elastic peak of the x-ray scattering in CrO_2 has been observed to be more pronounced than in usual Cr compounds, e.g. in elemental chromium. The authors of this work have put forward some qualitative arguments that the NQP states may give larger contributions to resonant x-ray scattering than the usual itinerant electron states. Equation (25) makes a quantitative estimation for this effect.

5. Transport properties

Transport properties of the HMF are the subject of numerous experimental investigations (see, e.g., recent works on CrO_2 [66], NiMnSb [67], and the reviews in [2, 68, 69]). At the same time, a theoretical interpretation of these results is still problematic. Concerning electronic scattering mechanisms, the most important difference between the HMF and 'standard' itinerant electron ferromagnets like iron or nickel is the absence of one-magnon spin-flip scattering processes in the former case since the states with only one spin projection are present at the Fermi level [2]. This seems to be confirmed by comparing experimental data on the resistivity of Heusler alloys TMnSb (T = Ni, Co, Pt, Cu, Au) and PtMnSn [31], the T^2-contribution from one-magnon processes for half-metallic systems (T = Ni, Co, Pt) not really being picked out.

Two-magnon scattering processes were considered many years ago, the temperature dependence of resistivity obtained being $T^{7/2}$ [70]. At low enough temperatures this result fails and should be replaced by $T^{9/2}$ [71]; the reason for this is compensation of transverse and longitudinal contributions in the long-wavelength limit, which is a consequence of the rotational symmetry of the s–d exchange Hamiltonian [72, 73]. Recently, a general interpolation theory has been formulated [75]. Here we present the main results of this work with a special emphasis on the NQP effects.

To consider the renormalization of the longitudinal processes in higher orders in I we have to eliminate from the Hamiltonian the terms which are linear in the magnon operators by using the canonical transformation [72]. Then the effective Hamiltonian takes the form

$$\widetilde{\mathcal{H}} = \mathcal{H}_0 + \tfrac{1}{2} \sum_{\mathbf{kqp}\sigma} (\mathcal{A}^{\sigma}_{\mathbf{kq}} + \mathcal{A}^{\sigma}_{\mathbf{k+q-p,q}}) c^{\dagger}_{\mathbf{k}\sigma} c_{\mathbf{k+q-p}\sigma} b^{\dagger}_{\mathbf{q}} b_{\mathbf{p}}, \tag{26}$$

where the zero-order Hamiltonian includes non-interacting electrons and magnons with the spin splitting $\Delta = 2IS$ being included in $\mathcal{H}_0$, and

$$\mathcal{A}^{\sigma}_{\mathbf{kq}} = \sigma I \frac{t_{\mathbf{k+q}} - t_{\mathbf{k}}}{t_{\mathbf{k+q}} - t_{\mathbf{k}} + \sigma\Delta} \tag{27}$$

is the s–d scattering amplitude, which vanishes at $q \to 0$ and thereby takes properly into account the symmetry of the electron–magnon interaction. A more general interpolation expression for the effective amplitude which does not assume the smallness of $|I|$ or $1/S$ was obtained in [73] within a variational approach.

The conductivity can be calculated in the Kubo formalism [76] to find an expression for the transport relaxation time τ ($I > 0, \sigma = \uparrow$; see details in [75]):

$$\frac{1}{\tau} = \frac{\pi}{4T}\sum_{\mathbf{kk'q}}(v^x_{\mathbf{k}} - v^x_{\mathbf{k'}})^2(\mathcal{A}^{\uparrow}_{\mathbf{kq}} + \mathcal{A}^{\uparrow}_{\mathbf{k'},\mathbf{q}-\mathbf{k'}+\mathbf{k}})^2 N_{\mathbf{q}}(1 + N_{\mathbf{q}-\mathbf{k'}+\mathbf{k}})n_{\mathbf{k}\uparrow}(1 - n_{\mathbf{k'}\uparrow})$$
$$\times\, \delta(t_{\mathbf{k'}} - t_{\mathbf{k}} - \omega_{\mathbf{q}} + \omega_{\mathbf{q}-\mathbf{k'}+\mathbf{k}}) \Big/ \sum_{\mathbf{k}}(v^x_{\mathbf{k}})^2\delta(t_{\mathbf{k}\uparrow}). \tag{28}$$

Averaging over angles of the vector $\mathbf{k}$ leads us to the final result $1/\tau \propto I^2\Phi$ with

$$\Phi = \sum_{\mathbf{pq}} f_{\mathbf{pq}} \frac{\beta(\omega_{\mathbf{p}} - \omega_{\mathbf{q}})|\mathbf{p} - \mathbf{q}|}{\exp\beta\omega_{\mathbf{p}} - \exp\beta\omega_{\mathbf{q}}}(1 + N_{\mathbf{q}})(1 + N_{\mathbf{p}}), \tag{29}$$

where $f_{\mathbf{pq}} = 1$ for $p, q \gg q_0$ and

$$f_{\mathbf{pq}} = \frac{[\mathbf{p}\times\mathbf{q}]^2}{(\mathbf{p}-\mathbf{q})^2 q_0^2} \qquad (p, q \ll q_0). \tag{30}$$

The wavevector q_0 determines the boundary of a region where the $\mathbf{q}$ dependence of the amplitude become important, so that $t(\mathbf{k}+\mathbf{q}) - t(\mathbf{k}) \simeq \Delta$ at $q \simeq q_0$ and the simple perturbation theory fails. In the one-band model of HMF where $E_{\mathrm{F}} < \Delta$ one has $q_0 \sim \sqrt{\Delta/W}$ (W is the conduction bandwidth, the lattice constant is put to unity) [72]. Generally speaking, q_0 may be sufficiently small provided that the energy gap is much smaller than W, which is the case for real HMF systems (e.g. in the hybridization model of the HMF spectrum (10)). It is important that similar crossover temperatures appear in the temperature dependence of the spin polarization (see, e.g., equation (17)). This means that temperature dependences of both spin polarization and transport properties can be changed at low enough temperatures within the spin-wave temperature region.

One has to bear in mind that each power of p or q in (29) yields the $T^{1/2}$ factor for the temperature dependence of resistivity. At very low temperatures $T < T^*$ small quasimomenta $p, q < q_0$ give a major contribution to the integrals. Then the temperature dependence of resistivity is equal to $\rho(T) \propto (T/T_{\mathrm{C}})^{9/2}$. Such a dependence was obtained in the narrow-band case (double-exchange model with large $|I|$), where the scale T^* is absent [74]. At the same time, for $T > T^*$ the function $f_{\mathbf{pq}}$ in equation (29) can be replaced by unity, leading to $\rho(T) \propto (T/T_{\mathrm{C}})^{7/2}$, in agreement with the old results [70].

According to calculations presented here, the NQP states do *not* contribute to the temperature dependence of the resistivity for pure HMF. An opposite conclusion was made by Furukawa [77] and related to an anomalous T^3 dependence in the resistivity. However, this calculation was not based on a consistent use of the Kubo formula and, in our opinion, can hardly be justified. In contrast, *impurity* contributions to transport properties in the presence of potential scattering are determined mainly by the NQP states [2, 22]. To second order in the impurity potential $\mathcal{U}$ we derive, after neglecting vertex corrections and averaging over impurities, for the transport relaxation time

$$\delta\tau^{-1}_{\mathrm{imp}}(E) = -2\mathcal{U}^2\,\mathrm{Im}\sum_{\mathbf{p}} G^{(0)}_{\mathbf{p}\sigma}(E) \tag{31}$$

where $G^{(0)}_{\mathbf{k}\sigma}(E)$ is the exact Green's function for the ideal crystal. Thus the contributions under consideration are determined by the energy dependence of the density of states $N(E)$ for the interacting system near the Fermi level. The most non-trivial dependence comes from the NQP (incoherent) states with the spin projection $-\sigma = -\,\mathrm{sgn}\, I$, which are present near E_{F}. Near the Fermi level the NQP contribution is determined by the magnon density of states $g(\omega)$ and follows a power law,

$$\delta N_{\mathrm{incoh}}(E) \propto \int_0^{\sigma E} \mathrm{d}\omega\, g(\omega) \propto |E|^{\mu}\theta(\sigma E) \qquad (|E| \ll \overline{\omega}). \tag{32}$$

Here $\theta(x)$ is the step function, E is referred to E_F; we have $\mu = 3/2$ and $\mu = 1$ for 3D and 2D cases, respectively. The corresponding correction to resistivity reads

$$\frac{\delta\rho_{\rm imp}(T)}{\rho^2} = -\delta\sigma_{\rm imp}(T)$$
$$\propto -\mathcal{U}^2 \int {\rm d}E \left(-\frac{\partial f(E)}{\partial E}\right) \delta N_{\rm incoh}(E) \propto T^{\mu}. \tag{33}$$

The contribution of the order of T^{μ} with $\mu \simeq 1.65$ (which is not too far from $3/2$) was observed in the temperature dependence of the resistivity for NiMnSb [67]. The incoherent contribution to magnetoresistivity is given by

$$\delta\rho_{\rm imp}(T, H) \propto \omega_0 \partial \delta N_{\rm incoh}(\sigma T)/\partial T \propto \omega_0 T^{\mu-1}. \tag{34}$$

The correction to thermoelectric power, which is similar to (33), reads (cf [22]):

$$\delta\mathcal{Q}(T) \propto \frac{1}{T} \int {\rm d}E\, (-\partial f(E)/\partial E) E \delta N(E) \tag{35}$$

and yields the same temperature dependence.

To calculate the magnetoresistivity we take into account a gap in the magnon spectrum induced by the magnetic field, $\omega_{\mathbf{q}\to 0} = Dq^2 + \omega_0$. For large external magnetic field, H, in comparison with the anisotropy gap, ω_0 is proportional to H. At $T < T^*$ the resistivity is linear in magnetic field:

$$\rho(T, H) - \rho(T, 0) \propto -\omega_0 T^{7/2}/T_{\rm C}^{9/2}. \tag{36}$$

The situation at $T > T^*$ is more interesting since the quantity $\partial\Lambda/\partial\omega_0$ contains a logarithmic divergence with the cut-off at ω_0 or T^*. We have at $T > \omega_0, T^*$:

$$\delta\rho(T, H) \propto -\frac{T^3\omega_0}{[\max(\omega_0, T^*)]^{1/2}}. \tag{37}$$

Of course, at $T < \omega_0$ the resistivity is exponentially small. A negative H-linear magnetoresistance was observed recently in CrO_2 [66]. The incoherent contribution to magnetoresistivity is given by

$$\delta\rho_{\rm imp}(T, H) \propto \omega_0 \partial \delta N_{\rm incoh}(\sigma T)/\partial T \propto \omega_0\sqrt{T}. \tag{38}$$

Another useful tool to detect the NQP states is provided by tunnelling phenomena [78], in particular by the Andreev reflection spectroscopy for the HMF–superconductor tunnel junction [11]. A most direct way is the measurement of a tunnel current between two pieces of the HMF with opposite magnetization directions. To this end we consider a standard tunnelling Hamiltonian (see, e.g., [62], section 9.3):

$$\mathcal{H} = \mathcal{H}_{\rm L} + \mathcal{H}_{\rm R} + \sum_{\mathbf{kp}} (T_{\mathbf{kp}} c^{\dagger}_{\mathbf{k}\uparrow} c_{\mathbf{p}\downarrow} + {\rm h.c.}) \tag{39}$$

where $\mathcal{H}_{\rm L,R}$ are the Hamiltonians of the left (right) half-spaces, respectively, $\mathbf{k}$ and $\mathbf{p}$ are the corresponding quasimomenta, and spin projections are defined with respect to the magnetization direction of a given half-space (the spin is supposed to be conserving in the 'global' coordinate system). Carrying out standard calculations of the tunnelling current $\mathcal{I}$ in the second order in $T_{\mathbf{kp}}$ we obtain (cf [62])

$$\mathcal{I} \propto \sum_{\mathbf{kqp}} |T_{\mathbf{kp}}|^2 [1 + N_{\mathbf{q}} - f(t_{\mathbf{p}-\mathbf{q}})][f(t_{\mathbf{k}}) - f(t_{\mathbf{k}} + e\mathcal{V})]\delta(e\mathcal{V} + t_{\mathbf{k}} - t_{\mathbf{p}-\mathbf{q}} + \omega_{\mathbf{q}})$$

where $\mathcal{V}$ is the bias voltage. For $T = 0$ one has ${\rm d}\mathcal{I}/{\rm d}\mathcal{V} \propto \delta N_{\rm incoh}(e\mathcal{V})$.

A very efficient new experimental method is spin-polarized scanning tunnelling microscopy (STM) [14] which enables one to probe directly the spectral density with spin

resolution in magnetic systems. The spin-polarized STM should be able to probe the NQP states via their contribution to the differential tunnelling conductivity $d\mathcal{I}_\sigma/d\mathcal{V} \propto N_\sigma(e\mathcal{V})$. The above formulae are derived for the usual one-electron density of states at E_F, which is observed, say, in photoemission measurements. However, the factors which are present in the expression for the tunnelling current do not influence the temperature dependence, and therefore these results are valid for spin polarization from tunnelling conductance at zero bias in STM [12, 81]. Unlike photoemission spectroscopy which probes only occupied electron states, STM detects the states both above and below E_F, depending on the sign of bias.

Another interesting tool to probe the half-metallic nature is the investigation of nuclear magnetic relaxation (NMR). In HMF the one-magnon decay processes do not work, and the T-linear Korringa contribution to the longitudinal nuclear relaxation rate $1/T_1 \propto T N_\uparrow(E_F) N_\downarrow(E_F)$ is absent and two-magnon scattering processes should be considered. This contribution yields the temperature dependence $1/T_1 \propto T^{5/2}$ which distinguishes HMF and usual magnets [10].

6. Conclusions

To conclude, we have considered the peculiarities of the properties of half-metallic ferromagnets which are connected with the unusual electronic structure of these systems including NQP states. Further theoretical and experimental investigations would be of great importance, especially keeping in mind the possible role of HMF in applications [2–4].

Several experiments could be performed in order to clarify the impact of the NQP states on spintronics. Direct ways of observing the NQP states would imply the technique of BIS [27] (for the most frequent case of a minority-spin gap where the NQP states lie above E_F) or spin-polarized scanning tunnelling microscopy (SP-STM) [14]. In contrast with PES (photoelectron spectroscopy of the occupied states), which has to show a complete spin polarization in HMF, BIS spectra should demonstrate an essential depolarization of the states above E_F. $\mathcal{I}$–$\mathcal{V}$ characteristics of half-metallic tunnel junctions for the case of antiparallel spins are completely determined by NQP states [75, 79]. The spin-polarized STM should be able to probe these states which give the minority-spin contribution to the differential tunnelling conductivity $d\mathcal{I}/d\mathcal{V}$ [12, 62, 80]. In particular, SP-STM with positive bias voltage can detect the opposite-spin states just above the Fermi level for a surface of HMF like CrO_2. Andreev reflection spectroscopy for the tunnel junction superconductor–HMF [11] can also be used in searching for experimental evidence of NQP effects. These experimental measurements will be of crucial importance for the theory of spintronics in any tunnelling devices with HMF. Since ferromagnetic semiconductors can be considered as a peculiar case of HMF [2], an account of these states can be important for a proper description of spin diodes and transistors [82].

Acknowledgments

The research described was supported by the Stichting voor Fundamenteel Onderzoek der Materie (FOM), the Netherlands Organization for Scientific Research (Grant NWO 047.016.005) and the Russian Basic Research Foundation (Grant 4640.2006.2).

References

[1] de Groot R A, Mueller F M, van Engen P G and Buschow K H J 1983 *Phys. Rev. Lett.* **50** 2024
[2] Irkhin V Yu and Katsnelson M I 1994 *Usp. Fiz. Nauk* **164** 705
Irkhin V Yu and Katsnelson M I 1994 *Phys.—Usp.* **37** 659 (Engl. Transl.)

[3] Pickett W E and Moodera J 2001 *Phys. Today* **54** (5) 39
[4] Prinz G A 1998 *Science* **282** 1660
[5] Park J H, Vescovo E, Kim H J, Kwon C, Ramesh R and Venkatesan T 1998 *Nature* **392** 794
[6] Nadgorny B, Mazin I I, Osofsky M, Soulen R J, Broussard P, Stroud R M, Singh D J, Harris V G, Arsenov A and Mukovskii Ya 2001 *Phys. Rev.* B **63** 184433
[7] Edwards D M and Hertz J A 1973 *J. Phys. F: Met. Phys.* **3** 2191
[8] Irkhin V Yu and Katsnelson M I 1983 *Fiz. Tverd. Tela* **25** 3383
Irkhin V Yu and Katsnelson M I 1983 *Sov. Phys.—Solid State* **25** 1947 (Engl. Transl.)
Irkhin V Yu and Katsnelson M I 1985 *J. Phys. C: Solid State Phys.* **18** 4173
[9] Katsnelson M I and Edwards D M 1992 *J. Phys.: Condens. Matter* **4** 3289
[10] Irkhin V Yu and Katsnelson M I 2001 *Eur. Phys. J.* B **19** 401
[11] Tkachov G, McCann E and Fal'ko V I 2001 *Phys. Rev.* B **65** 024519
[12] Irkhin V Yu and Katsnelson M I 2006 *Phys. Rev.* B **73** 104429
[13] Kevan S D 1992 *Angle-Resolved Photoemission: Theory and Current Applications* (Amsterdam: Elsevier)
[14] Wiesendanger R, Guentherodt H-J, Guentherodt G, Cambino R J and Ruf R 1990 *Phys. Rev. Lett.* **65** 247
[15] Chioncel L, Katsnelson M I, de Groot R A and Lichtenstein A I 2003 *Phys. Rev.* B **68** 144425
[16] Chioncel L, Arrigoni E, Katsnelson M I and Lichtenstein A I 2006 *Phys. Rev. Lett.* **96** 137203
[17] Chioncel L, Katsnelson M I, de Wijs G A, de Groot R A and Lichtenstein A I 2005 *Phys. Rev.* B **71** 085111
[18] Chioncel L, Mavropoulos Ph, Lezaic M, Blügel S, Arrigoni E, Katsnelson M I and Lichtenstein A I 2006 *Phys. Rev. Lett.* **96** 197203
[19] Chioncel L, Allmaier H, Yamasaki A, Daghofer M, Arrigoni E, Katsnelson M I and Lichtenstein A I 2007 *Phys. Rev.* B **75** 140406
[20] Nozieres P 1964 *Theory of Interacting Fermi Systems* (New York: Benjamin)
Pines D and Nozieres P 1966 *The Theory of Quantum Liquids* (New York: Benjamin)
[21] Irkhin V Yu and Katsnelson M I 1990 *J. Phys.: Condens. Matter* **2** 7151
[22] Irkhin V Yu, Katsnelson M I and Trefilov A V 1989 *Physica* C **160** 397
Irkhin V Yu, Katsnelson M I and Trefilov A V 1994 *Zh. Eksp. Teor. Fiz.* **105** 1733
Irkhin V Yu, Katsnelson M I and Trefilov A V 1994 *Sov. Phys.—JETP* **78** 936 (Engl. Transl.)
[23] Nagaoka Y 1966 *Phys. Rev.* **147** 392
[24] Irkhin V Yu and Zarubin A V 2004 *Phys. Rev.* B **70** 035116
[25] Auslender M I and Irkhin V Yu 1985 *J. Phys. C: Solid State Phys.* **18** 3533
[26] Kobayashi K-I, Kimura T, Sawada H, Terakura K and Tokura Y 1998 *Nature* **395** 677
[27] Unguris J, Seiler A, Celotta R J, Pierce D T, Johnson P D and Smith N V 1982 *Phys. Rev. Lett.* **49** 1047
[28] Edwards D M 1983 *J. Phys. C: Solid State Phys.* **16** L327
[29] Auslender M I and Irkhin V Yu 1984 *Solid State Commun.* **50** 1003
[30] Kisker E, Baum G, Mahan A, Raith W and Reihl B 1978 *Phys. Rev.* B **18** 2256
[31] Otto M J, van Woerden R A M, van der Valk P J, Wijngaard J, van Bruggen C F and Haas C 1989 *J. Phys.: Condens. Matter* **1** 2351
[32] Skomski R and Dowben P A 2002 *Europhys. Lett.* **58** 544
[33] de Wijs G A and de Groot R A 2001 *Phys. Rev.* B **64** 020402
[34] Weht R and Pickett W E 1999 *Phys. Rev.* B **60** 13006
[35] Shishidou T, Freeman A J and Asahi R 2001 *Phys. Rev.* B **64** 180401
[36] Galanakis I, Dederichs P H and Papanikolaou N 2002 *Phys. Rev.* B **66** 134428
[37] Korotin M A, Anisimov V I, Khomskii D I and Sawatzky G A 1998 *Phys. Rev. Lett.* **80** 4305
[38] Anisimov V I, Poteryaev A I, Korotin M A, Anokhin A O and Kotliar G 1997 *J. Phys.: Condens. Matter* **9** 7359
[39] Lichtenstein A I and Katsnelson M I 1998 *Phys. Rev.* B **57** 6884
Katsnelson M I and Lichtenstein A I 1999 *J. Phys.: Condens. Matter* **11** 1037
[40] Georges A, Kotliar G, Krauth W and Rozenberg M 1996 *Rev. Mod. Phys.* **68** 13
[41] Hohenberg P and Kohn W 1964 *Phys. Rev.* **136** B864
[42] Kohn W and Sham L J 1965 *Phys. Rev.* **140** A1133
[43] von Barth U and Hedin L 1972 *J. Phys. C: Solid State Phys.* **5** 1629
[44] Lichtenstein A I and Katsnelson M I 2001 *Band Ferromagnetism. Ground State and Finite-Temperature Phenomena* (*Springer Lecture Notes in Physics*) ed K Barbeschke, M Donath and W Nolting (Berlin: Springer)
Lichtenstein A I, Katsnelson M I and Kotliar G 2002 *Electron Correlations and Materials Properties 2* ed A Gonis, N Kioussis and M Ciftan (Dordrecht: Kluwer–Academic/Plenum) p 428
[45] Held K, Nekrasov I A, Keller G, Eyert V, Bluemer N, McMahan A K, Scalettar R T, Pruschke T, Anisimov V I and Vollhardt D 2002 *Quantum Simulations of Complex Many-Body Systems: From Theory to Algorithms* (*NIC Series* vol 10) ed J Grotendorst, D Marx and A Muramatsu (Juelich: NIC) p 175

[46] Kotliar G and Savrasov S Y 2001 *New Theoretical Approaches to Strongly Correlated Systems* ed A M Tsvelik (Dordrecht: Kluwer–Academic)
[47] Kotliar G, Savrasov S, Haule K, Oudovenko V, Parcolet O and Marianetti C 2006 *Rev. Mod. Phys.* **78** 865
[48] Chadov S, Minár J, Ebert H, Perlov A, Chioncel L, Katsnelson M I and Lichtenstein A I 2006 *Phys. Rev.* B **74** 140411
[49] Jarrell M 1992 *Phys. Rev. Lett.* **69** 168
[50] Andersen O K, Jepsen O and Krier G 1994 *Lectures on Methods of Electronic Structure Calculations* ed V Kumar, O K Andersen and A Mookerjee (Singapore: World Scientific) p 63
Andersen O K and Saha-Dasgupta T 2000 *Phys. Rev.* B **62** R16219
[51] Vitos L, Skriver H L, Johansson B and Kollár J 2000 *Comput. Mater. Sci.* **18** 24
[52] Chioncel L, Vitos L, Abrikosov I A, Kollár J, Katsnelson M I and Lichtenstein A I 2003 *Phys. Rev.* B **67** 235106
[53] Katsnelson M I and Lichtenstein A I 2002 *Eur. Phys. J.* B **30** 9
[54] Bickers N E and Scalapino D J 1989 *Ann. Phys.* **193** 206
[55] Galitski V M 1958 *Zh. Eksp. Teor. Fiz.* **34** 115
Galitski V M 1958 *Zh. Eksp. Teor. Fiz.* **34** 1011
Kanamori J 1963 *Prog. Theor. Phys.* **30** 275
[56] Anisimov V I and Gunnarsson O 1991 *Phys. Rev.* B **43** 7570
[57] Irkhin V Yu and Katsnelson M I 2005 *Eur. Phys. J.* B **43** 479
[58] Yarmoshenko Yu M, Katsnelson M I, Shreder E I, Kurmaev E Z, Slebarski A, Plogmann S, Schlathoelter T, Braun J and Neumann M 1998 *Eur. Phys. J.* B **2** 1
[59] Yablonskikh M V, Yarmoshenko Y M, Grebennikov V I, Kurmaev E Z, Butorin S M, Duda L-C, Nordgren J, Plogmann S and Neumann M 2001 *Phys. Rev.* B **63** 235117
[60] Kurmaev E Z, Moewes A, Butorin S M, Katsnelson M I, Finkelstein L D, Nordgren J and Tedrow P M 2003 *Phys. Rev.* B **67** 155105
[61] Wessely O, Roy P, Aberg D, Andersson C, Edvardsson S, Karis O, Sanyal B, Svedlindh P, Katsnelson M I, Gunnarsson R, Arvanitis D, Bengone O and Eriksson O 2003 *Phys. Rev.* B **68** 235109
[62] Mahan G D 1990 *Many-Particle Physics* (New York: Plenum)
[63] Ebert H 1996 *Rep. Prog. Phys.* **59** 1665
[64] Gel'mukhanov F and Agren H 1994 *Phys. Rev.* A **49** 4378
[65] Sokolov O B, Grebennikov V I and Turov E A 1977 *Phys. Status Solidi* b **83** 383
[66] Rabe M, Pommer J, Samm K, Oezyilmaz B, Koenig C, Fraune M, Ruediger U, Guentherodt G, Senz S and Hesse D 2002 *J. Phys.: Condens. Matter* **14** 7
[67] Borca C N, Komesu T, Jeong H-K, Dowben P A, Ristoiu D, Hordequin Ch, Nozieres J P, Pierre J, Stadler S and Idzerda Y U 2001 *Phys. Rev.* B **64** 052409
[68] Ziese M 2002 *Rep. Prog. Phys.* **65** 143
[69] Nagaev E L 2001 *Phys. Rep.* **346** 388
[70] Roesler M 1965 *Phys. Status Solidi* **8** K31
Hartman-Boutron F 1965 *Phys. Kond. Mater.* **4** 114
[71] Lutovinov V S and Reizer M Yu 1979 *Zh. Eksp. Teor. Fiz.* **77** 707
[72] Grigin A P and Nagaev E L 1974 *Phys. Status Solidi* b **61** 65
[73] Auslender M I, Katsnelson M I and Irkhin V Yu 1983 *Physica* B **119** 309
[74] Kubo K and Ohata N 1972 *J. Phys. Soc. Japan* **33** 21
[75] Irkhin V Yu and Katsnelson M I 2002 *Eur. Phys. J.* B **30** 481
[76] Nakano H 1957 *Prog. Theor. Phys.* **17** 145
Mori H 1965 *Prog. Theor. Phys.* **34** 399
[77] Furukawa N 2000 *J. Phys. Soc. Japan* **69** 1954
[78] Auslender M I and Irkhin V Yu 1985 *Solid State Commun.* **56** 703
[79] McCann E and Fal'ko V I 2003 *Phys. Rev.* B **68** 172404
[80] Meir Y and Wingreen N S 1992 *Phys. Rev. Lett.* **68** 2512
[81] Ukraintsev V A 1996 *Phys. Rev.* B **53** 11176
[82] Flatte M E and Vignale G 2001 *Appl. Phys. Lett.* **78** 1273